ROMANIAN JOURNAL OF INFORMATION SCIENCE AND TECHNOLOGY
Volume **14**, Number 4, 2011, 299–308

Nanostructured Film of Indium Phosphide as Biosensor in 1D Array Electrowetting System

L. SIRBU[1], I. VODA[2], D. ESINENCO[3], S. GANGAN[3], R. MULLER[4], R. VOICU[4], M. DANILA[4], L. GHIMPU[1], I. M. TIGINYANU[1,3], V. URSAKI[3,5]

[1]Institute of Electronic Engineering and Nanotechnologies *"D. Ghitu"*, 3/3, Academiei str., MD-2028 Chisinau, Moldova

[2]Institute of Chemistry of the Academy of Sciences of Moldova, Academiei str., MD-2028 Chisinau

[3]Moldova Technical University of Moldova, 168, Stefan cel Mare str., MD-2004 Chisinau, Moldova

[4]National Institute for R&D in Microtechnologies - IMT Bucharest, Erou Iancu Nicolae 126 A Str., Romania

[5]Institute of Applied Physics, Academy of Science of Moldova, 5, Academiei str., MD-2028 Chisinau, Moldova

E-mail: sirbu_lilian@yahoo.de

Abstract. We demonstrated the fabrication of complex nanostructured InP membranes with porous compact packed structure that have been cut during electrochemical etching in the same anodic process. The membranes were filled with optically transparent compounds. The compounds deposition in the porous structure was carried out in diverse conditions: temperature, light, bake. The monomer was incorporated into the porous layer from a $[Zn(C_3N_2(C_6H_5)_2NO_2)_2(CH_3OH)_2]$ and $[Ni(C_3N_2(C_6H_5)_2NO_2)_2(CH_3OH)_2]$ solution. We considered the covering of the nanoporous film and filling the pores with coordination compounds imprinted with nano metallic particles in order to stabilize and adjust the sensor characteristics for specific biological samples. Also we designed and fabricated lab-on-a-chip devices based on Si which can be used for transporting bio-samples to the detector by means of electrowetting method. The experimental study and simulations based on Finite Element Model (FEM) and Finite-difference time-domain Model (FDTD) show also that

the obtained materials are promising for nonlinear optical applications, in particular for the development of electrowetting systems for MEMS, MOEMS, etc.

1. Introduction

Electrowetting has become one of the most widely used tools for manipulating tiny amounts of liquids on surfaces. Electrowetting involves application of electrical potential across a liquid/dielectric/electrode capacitor, a charge-induced imbalance of forces near the liquid/dielectric contact line, and a resulting decrease in the observed liquid contact angle. Quite a lot of electrowetting technologies are already on their way to commercialization, including those used for liquid lenses [1], lab-on-chip [2], and electronic displays [3]. Investigation of electrowetting on superhydrophobic surfaces has been a more recent research topic. Thereby electrowetting can change proprieties of surface from hydroscopic to hydrophobic and back by using applied voltage on pads (Fig. 1).

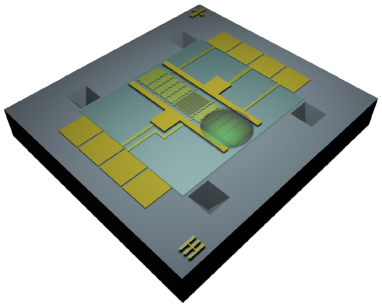

Fig. 1. Electrowetting system based on silicon substrate.

On the other hand, the fabrication of sensor needs [4] special proprieties of the used films as they have to absorb as much as possible the incident light and focus it on the biosample (Fig. 2). That was the reason to fabricate a porous membrane with variable diameter of pores and to study the scattering light in near field region.

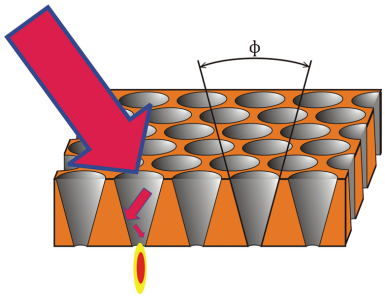

Fig. 2. Model for cone – shaped pores.

A capability to focus beams of light to small-sized spots is essential for development of proposed nanoscale optical biosensor based on near-field optical interactions [5, 6]. This feature will have contribution to the development of nanophotonic devices, including precision scanner for bio-sample integrated in electrowetting system [7, 8].

An emerging branch of photonics, called "plasmonics", aims at using nanostructured materials that support "surface plasmons" for these purposes. Plasmonics can potentially achieve highly complex miniaturized devices by controlling and manipulating light on the nanometer scale [9–11]. Several plasmonic devices including filters [9], waveguides [9, 11], polarizers [12], and nanoscopic light source [13] have been demonstrated. Geometrically ordered metal nanostructures, such as periodic arrays of metal nanoparticles, arrays of holes in metal films, and metal nano-wire meshes are nowadays fabricated for tunable optical responses with frequency-, polarization-, and angle-selective enhancements. These materials may also be developed as robust photonic crystals with large and scaleable band gaps due to their negative dielectric permittivities.

Consequently, for better control the proprieties of porous membrane we considered to deposit the Ag nanodots by electrochemical methods in side InP porous nanostucture. In this case we studied also the surface plasmon resonance effect on intern surface of nanoimprinted InP [14].

2. Experimental setup

2.1. Sample fabrication and morphology

We used crystalline (100) oriented substrates of S-doped n-InP with 500 μm thickness (prior to anodic etching) and free electron concentration of 1.3×10^{18} cm^{-3}. The anodization was performed in an electrochemical double cell Fig. 3 [15].

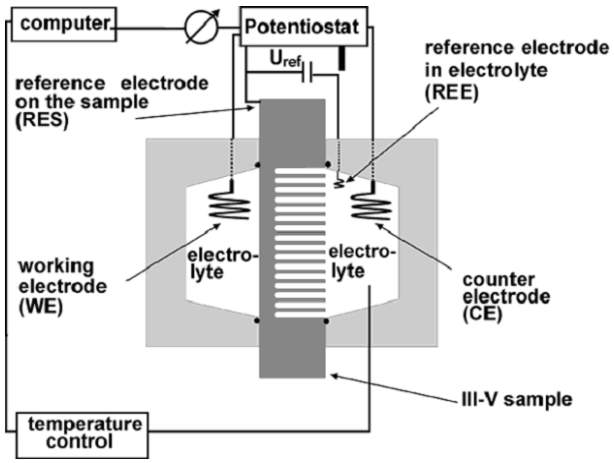

Fig. 3. The experimental set-up used for anodization of III–V compounds.

A four-electrode configuration was used: a Pt reference electrode in the elec-

trolyte, a Pt reference electrode on the sample, a Pt counter electrode, and a Pt working electrode. The temperature was kept constant with a thermostat. The electrolyte was pumped continuously through both parts of the double cell with the help of a peristaltic pump, Fig. 3 [15]. All equipment involved in the experiments was computer-controlled.

The area of the sample exposed to the electrolyte was 0.5 cm^2. The anodic etching was carried out in 5% HCl aqueous solution at room temperature in potentiostatic regime with the following range of values for obtaining gradient of diameter of pores: the applied voltage linearly and exponentially decreases from 8.0 to 1.0 that leads to changing degrees of porosity with depth. To have a thin porous film, we applied a shock pulse of bias from the potentiostat. The first pulse was used to remove the disordered layer of the porous structure (see [16]) and the next pulses were applied to fabricate films with ordered pores which were afterwards used in our experiments (see Fig. 4).

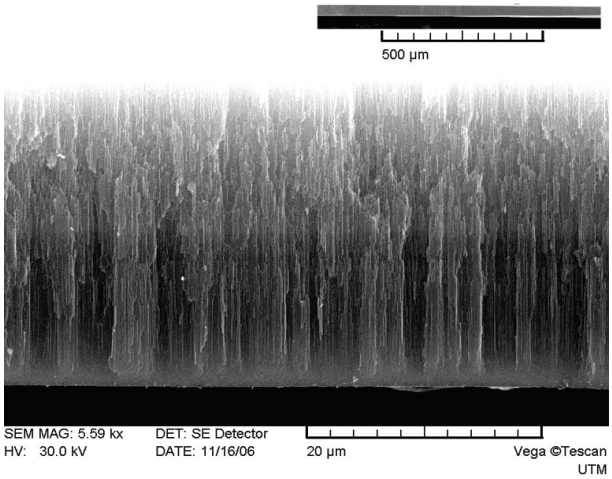

Fig. 4. SEM image of porous InP film.
The inset shows a smaller magnification.

Further details of the anodic etching process can be found in [15]. A TESCAN scanning electron microscope equipped with an Oxford Instruments INCA energy dispersive X-ray (EDX) system was used to analyze the morphology and chemical composition of the porous samples.

3.2. Electrodeposition of Ag nanodots

Ag nanoparticles have been deposited electrochemically on the porous surface as well as inside porous templates using an $AgNO_3$ aqueous solution [17]. The deposition was carried out with the application of 4 V pulses with the width of 100 µsec and frequency of 0.5 sec. The size and the density of Ag nanoparticles were controlled by the conditions of electrochemical deposition and the subsequent thermal treatment.

The deposition during 2 minutes followed by thermal treatment at 400°C during 1 hour leads to the formation of Ag particles as schematically illustrated in reference Fig. 5 [16, 18, 19].

3.3. Synthesize of coordination compounds

Coordination compounds with structural formula $[Zn(C_3N_2(C_6H_5)_2NO_2)_2(CH_3OH)_2]$ and $[Ni(C_3N_2(C_6H_5)_2NO_2)_2(CH_3OH)_2]$ have been synthesized and characterized by X-ray crystallography (see Fig. 6 ref. [16]). These complexes have pseudopolimeric structures being connected to each other by hydrogen bonding (Fig. 5). This behavior made possible the introduction of these complexes in porous *n*-InP membranes. The complex deposition in the porous structure was carried out in a dark room. The monomers were incorporated into the porous layer from $Zn(C_3N_2(C_6H_5)_2NO_2)_2(CH_3OH)_2$:$C_3H_6O$ and $Ni(C_3N_2(C_6H_5)_2NO_2)_2(CH_3OH)_2$:$C_3H_6O$ solutions. Afterwards, the samples were dried for several days at room temperature. The morphology of the monomer nanowires in an InP template is illustrated in reference [16, 20].

The EDX analysis of coordination compounds demonstrates that they have fully filled the nanostructured template of n-InP along the entire depth of pores.

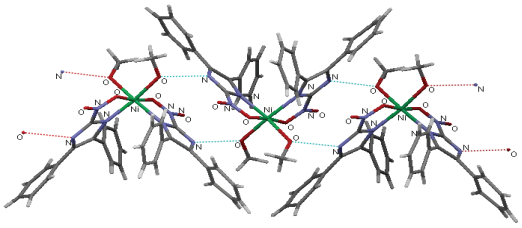

Fig. 5. Hydrogen bonding inside $[Ni(C_3N_2(C_6H_5)_2NO_2)_2(CH_3OH)_2]$ structure.

Scattering/reflectance signal was measured at wavelength 531 nm. A cw Nd:LSB microchip solid state laser was directed at incident angle α, the spot size of the beam at the sample was $\sim$2 mm. The scattered light was collected at varying angle β and guided to a detector (LN/CCD-1152-E 16-bit CCD array, Princeton Instruments). All measurements were performed at room temperature [21].

It was observed from scattering angular diagrams [22], that for some of samples there is a mirror reflection of the incident radiation and a partial dispersion. Other structures disseminate completely the incident radiation.

3.4. Design and fabrication of electrowetting system

We have integrated the sensing surface (thin film) into a lab on chip device [23]. The structure was formed using standard Si wafer technology: a set of golden electrodes were realized on high quality hydrophobic oxide, on the bottom of a microfluidic channel (configured in SU8 polymer) allowing electrowetting process to take place. The measurement and manipulation pads are connected to a printed circuit board developed on the basis of an AVR microcontroller and a high sensitivity low noise

operational amplifier. The measured characteristics are saved and processed using standard data processing software on the PC (see 3.5 part).

A voltage (V) is applied between the embedded electrode (pad) and the liquid droplet on the dielectric layer, the solid-liquid interfacial tension decreases and it reduces the contact angle from θ_0 to θ_V. If an array of the embedded electrode is patterned, the droplet can move to the activated area when a partial area of the droplet base is activated by controlling a part of the embedded electrode array. Then the electrowetting on dielectric (EWOD) device can be used to manipulate droplets for dispensing, transporting, splitting, merging, and mixing.

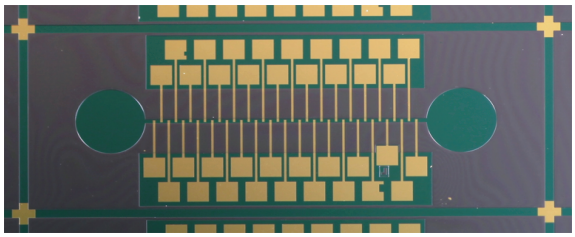

Fig. 6. Optical microscope image of the designed microchannel chip.

3.5. Controller of electrowetting system

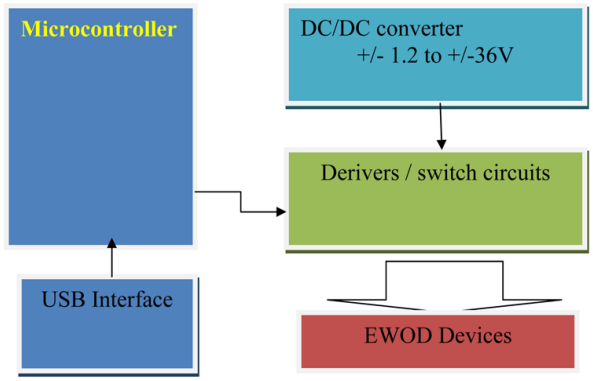

Fig.7. Block diagram of driving system for EWOD devices.

Lippmann-Young equation [24] shows the relationship between the contact angle change and the applied voltage through the dielectric layer, depending on the liquid-vapor interfacial tension and dielectric properties, as follows:

$$\cos\theta_V = \theta_0 + \frac{\varepsilon_0 \varepsilon_r}{2\gamma_{lv} d} V^2$$

where ε_0 is the permittivity of free space, ε_r is the relative permittivity of the dielectric, γ_{lv} is the liquid-vapor interfacial tension, and d is the thickness of the dielectric layer. According to this equation, a thinner dielectric layer with a high permittivity is desired to lower the driving voltage.

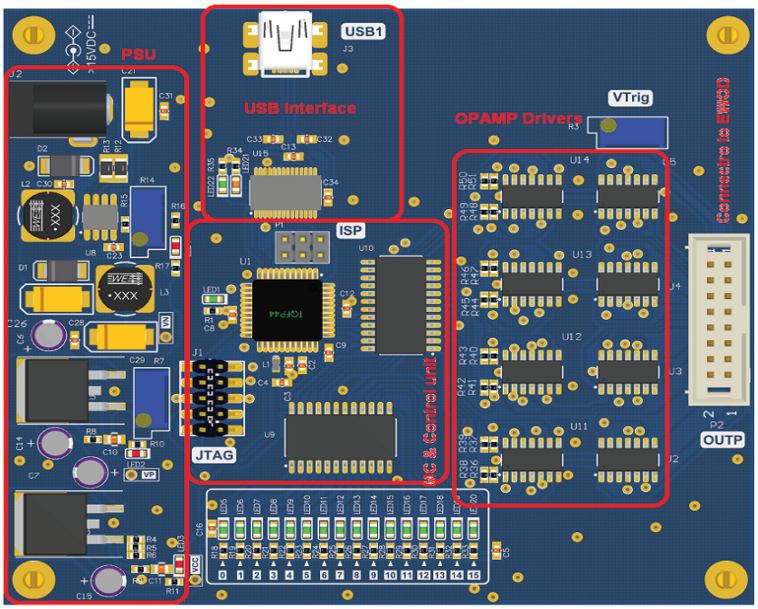

Fig. 8. PCB view of driving system for EWOD devices.

4. Simulation model for bio applications

One can see in Fig. 9 the distribution of the E component of the EM field along the cone – shaped pour. Regions in brown red show values of 3.6 a.u. which are 36 times higher that the incident irradiation intensity used in simulation. Moreover, the diameter where field intensity is higher than 0.5 of the maximum value is around quarter of the incident wavelength – the near field, whereas deeper it extends to the full wavelength diameter. Another sensitivity boost could be obtained by using different techniques for gathering molecules near the strong EM pikes. This can be achieved by using static E field or when irradiating the cones in case we obtain slow surface EM wave in the bottom pours region.

This simulation demonstrates that strong EM fields can take place when the metallic nanoparticles are deposited in the porous semiconductor templates. Thus, the semiconductor templates provide wide possibilities for the control of the surface plasmon resonance frequency of metallic nanoparticles, since the effective refractive index of the template can be varied from the value of the bulk material refractive index to values around 1 or even lower than 1 by tailoring the morphology and porosity, while the plasmon resonance frequency of metallic nanoparticles is highly sensitive to the refractive index of the medium they are incorporated into [25].

At the same time it was shown experimentally and theoretically that electromagnetic interaction of a nanoparticle with a flat dielectric surface leads to occurrence of an additional peak in the spectrum of Rayleigh scattering which is due to the contribution from quadrupole components in addition to the dipole ones. The results

of calculations are in a good correlation with experimental results. We considered the Rayleigh scattering of small metallic nanoparticles placed in the proximity of dielectric bodies. The simplest configuration of a semi-infinite dielectric space and a nanoparticle is considered. The optical properties of the metal are described by the Drude dielectric function [26].

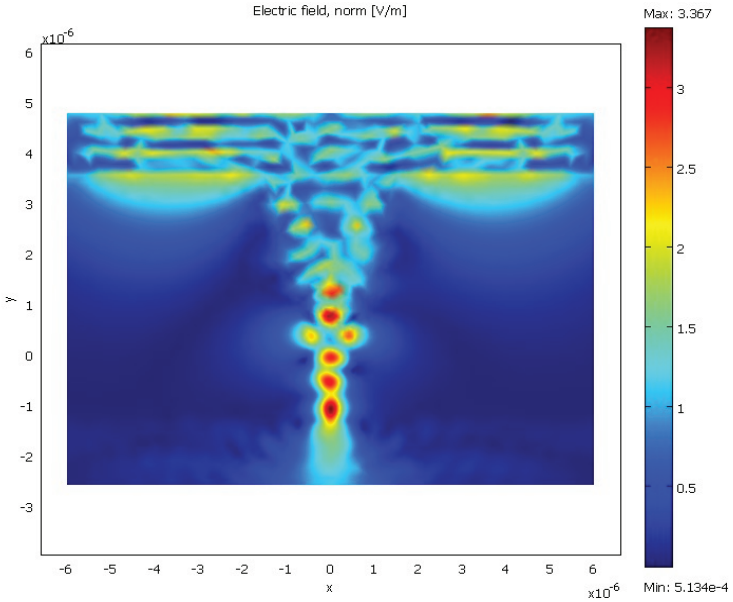

Fig. 9. EM field distribution for a single cone.

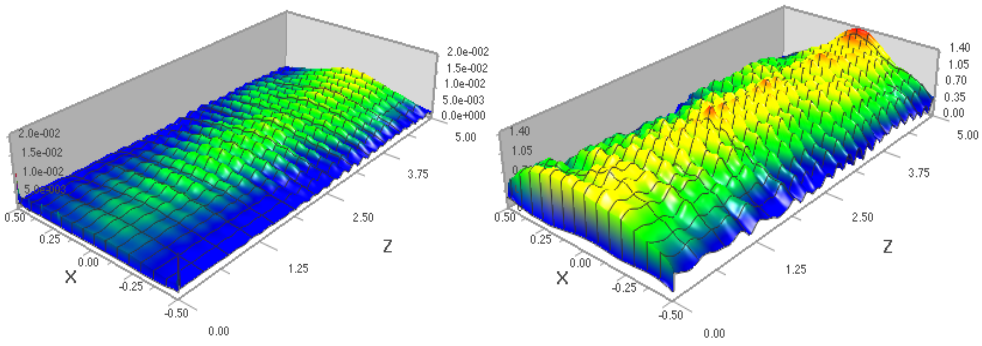

Fig. 10. FDTD simulation. (a) EM field distribution for a hundred pores cone-shaped; (b) EM field distribution for a hundred pores cone-shaped with Ag nanoparticles.

5. Conclusions

Some preliminary tests on different InP nano porous membranes filled with diverse metallic nano powder and polymers were successfully done. Pores with high uniformity in diameter and density distribution were obtained, using a low cost technology. The membranes indicate sensitivity in the IR and visible spectral diapasons. The goal to obtain interaction at nano scale level was achieved. Further work is to be done on handling the liquid samples using electrowetting manipulation with ultra short pulses in order to obtain fast repeated experiments with short and long controlled time of exposure of the sensing membrane to the bio environment.

Acknowledgments. This work was supported by Romanian Moldavian Bilateral project No. 10.820.05.23/RoA and 433 (2010-2012).

References

[1] Berge B., Peseux J., *Variable focal lens controlled by an external voltage: an application of electrowetting*, Euro. Phys. J. E., Soft Matter, **3**, p. 159, 2000.

[2] Pollack M. G., Fair R. B., Shenderov A. D., *Electrowetting-based actuation of liquid droplets for microfluidic applications*, Appl. Phys. Lett., **77**, p. 1725, 2000.

[3] Hayes R. A., Feenstra B. J., *Video-speed electronic paper based on electrowetting*, Nature, **425**, p. 383, 2003.

[4] Shen N. Y., Liu Z., Jacquot B. C., Minch B. A., Kan E. C., *Integration of chemical sensing and electrowetting actuation on chemoreceptive neuron MOS (C vMOS) transistors*, Sensors and Actuators B: Chemical, **102**, 1, pp. 35–43, 2004.

[5] Curto A. G., Manjavacas A., Garcia de Abajo F. J., *Near-field focusing with optical phase antennas*, Optics Express, Vol. **17**, No. 20, p. 17801, 2009.

[6] Fabre N., Lalouat L., Cluzel B., Mélique X., Lippens D., de Fornel F., Vanbésien O., *Optical Near-Field Microscopy of Light Focusing Through A Photonic Crystal Flat Lens*, A. Phys. Rev. Lett., **101**, p. 073901, 2008.

[7] Vanbesien O., Fabre N., Mélique X., Lalouat L., Cluzel B., de Fornel F., Lippens D., *Photonic Crystal Based Subwavelength Imaging and Cloaking Optical Devices*, Piers Online, Vol. **5**, No. 3, 2009.

[8] Lee J. Y., Hong B. H., Kim W. Y., Min S. K., Kim Y., Jouravlev M. V., Bose R., Kim K. S., Hwang I.-C., Kaufman L. J., Wong C. W., Kim P., Kim K. S., *Near-field focusing and magnification through self-assembled nanoscale spherical lenses*, Nature, Vol. **460**, 2009.

[9] Barnes W. L., Dereux A., Ebbesen T. W., *Surface plasmon subwavelength optics*, Nature, **424**, p. 824, 2003.

[10] Haynes C. L. et al., *Nanoparticle Optics: The Importance of Radiative Dipole Coupling in Two-Dimensional Nanoparticle Arrays*, J. Phys. Chem. B, **107**, p. 7337, 2003.

[11] Maier S. A. et al., *Local detection of electromagnetic energy transport below the diffraction limit in metal nanoparticle plasmon waveguides*, Nature Mater., **2**, p. 229, 2003.

[12] Haynes C. L., Van Duyne R. P., *Dichroic Optical Properties of Extended Nanostructures Fabricated Using Angle-Resolved Nanosphere Lithography*, Nano Lett., **3**, p. 939, 2003.

[13] Lezec H. J. et al, *Beaming Light from a Subwavelength Aperture*, Science, **297**, p. 820, 2002.

[14] Aizawa M., Buriak J. M., *Block Copolymer-Templated Chemistry on Si, Ge, InP, and GaAs Surfaces*, J. American Chemical Society, **127**, pp. 8932–8933, 2005.

[15] Langa S., Tiginyanu I. M., Carstensen J., Christophersen M., Foell H., *Self-organized growth of single crystals of nanopores*, Appl. Phys. Lett., **82**, p. 278, 2003.

[16] Sirbu L., Voda I., Esinenco D., Muller R., Voicu R., Danila M., Ghimpu L., Tiginyanu I. M., Ursaki V., *Nanostructured indium phosphide used in electrowetting system for biosensor applications*, CAS 2011, Oct. 17–19, Sinaia, Romania.

[17] Sirbu L., Sergentu V., Ursaki V., Tiginyanu I., Piredda G., Boyd R., *Surface Plasmon Resonance in Ag Nnoparticles Deposited Inside Porous GaP Templates*, CAS 2008, Oct. 13–15, Sinaia, Romania.

[18] Fang C., Foca E., Sirbu L., Carstensen J., Föll H., Tiginyanu I. M., *Formation of metal wire arrays via electrodeposition in pores of Si, Ge and III–V semiconductors*, Phys. Stat. Sol. (a), **204**, No. 5, pp. 1388–1393, 2007.

[19] Zdansky K., Zavadil J., Kacerovsky P., Kostka F., Lorincik J., Cernohorsky O., Muller M., Kostejn M., Fojtik A., *Films of Metal Nanoparticles Deposited on Semiconductors by Electrophoresis: Technology and Characterization*, Nanocon, 20–22.10.2009, Rožnov pod Radhoštem, Ceská Republika.

[20] Voda I., Sirbu L., Esinenco D., *MSCMP Chisinau 2010 Proceeding, 5^{th} International Conference on Materials Science and Condensed Matter Physics and Symposium "Electrical Methods of Materials Treatment" in memoriam of acad. Boris Lazarenko (1910–1979),* Chisinau, Moldova, September 13–17, 2010, pp. 210.

[21] Prislopski S., Tiginyanu I. M., Ghimpu L., Monaico E., Sirbu L., Zhukovsky S. V., Gaponenko S. V., *ICTON 2011*, Tu.C2.5.

[22] Prislopski S., Naumenko E. K., Tiginyanu I. M., Ghimpu L., Monaico E., Sirbu L., Gaponenko S. V., *Anomalous retroreflection from strongly absorbing nanoporous semiconductors*, Optics Letters, Vol. **36**, Issue 16, pp. 3227–3229, 2011.

[23] Esinenco D., Sirbu L., Voda I., Voicu R., Muller R., Gangan S., Ghimpu L., Tiginyanu I. M., Ursaki V., *EMRS Spring*, 2011, P.XVIb 8.

[24] *Encyclopedia of Microfluidics and Nanofluidics*, Editor-in-Chief: Dongqing Li, Vanderbilt University, p. 67, 2008.

[25] Sirbu L., Sergentu V., Ursaki V., Tiginyanu I., Piredda G., Boyd R. W., *International semiconductor conference*, October 13–15, Sinaia, Romania, p. 43, 2008.

[26] Sergentu V., Esinenco D., Sirbu L., Voda I., Voicu R., Tiginyanu I. M., Ursaki V., *CAS 2010, International Semiconductor Conference*, Sinaia, Romania, October 11–13, p. 65, 2010.